Discovery of tandem and interspersed segmental duplications using high throughput sequencing

Arda Soylev [1] ‡, Thong Le [2,3] ‡, Hajar Amini [4],
Can Alkan [1,5,6]* and Fereydoun Hormozdiari [2,7,8]*

[1] Department of Computer Engineering, Bilkent University, Ankara, 06800, Turkey

[2] UC-Davis Genome Center, University of California, Davis, CA, USA.

[3] Department of Computer Science, University of California, Davis, CA, USA.

[4] Department of Plant Biology, University of California, Davis, CA, USA.

[5] Bilkent-Hacettepe Health Sciences and Technologies Program, Ankara, 06800, Turkey

[6] Department of Computer Science, ETH Zürich, 8006, Switzerland

[7] Department of Biochemistry and Molecular Medicine, University of California, Davis, CA, USA.

[8] MIND Institute, University of California, Davis, CA, USA.

Abstract

Motivation: Several algorithms have been developed that use high throughput sequencing technology to characterize structural variations. Most of the existing approaches focus on detecting relatively simple types of SVs such as insertions, deletions, and short inversions. In fact, complex SVs are of crucial importance and several have been associated with genomic disorders. To better understand the contribution of complex SVs to human disease, we need new algorithms to accurately discover and genotype such variants. Additionally, due to similar sequencing signatures, inverted duplications or gene conversion events that include inverted segmental duplications are often characterized as simple inversions; and duplications and gene conversions in direct orientation may be called as simple deletions. Therefore, there is still a need for accurate algorithms to fully characterize complex SVs and thus improve calling accuracy of more simple variants.

Results: We developed novel algorithms to accurately characterize tandem, direct and inverted interspersed segmental duplications using short read whole genome sequencing data sets. We integrated these methods to our TARDIS tool, which is now capable of detecting various types of SVs using multiple sequence signatures such as read pair, read depth and split read. We evaluated the prediction performance of our algorithms through several experiments using both simulated and real data sets. In the simulation experiments, using a 30× coverage TARDIS achieved 96% sensitivity with only 4% false discovery rate. For experiments that involve real data, we used two haploid genomes (CHM1 and CHM13) and one human genome (NA12878) from the Illumina Platinum Genomes set. Comparison of our results with orthogonal PacBio call sets from the same genomes revealed higher accuracy for TARDIS than state of the art methods. Furthermore, we showed a surprisingly low false discovery rate of our approach for discovery of tandem, direct and inverted interspersed segmental duplications prediction on CHM1 (less than 5% for the top 50 predictions).

Availability: TARDIS source code is available at https://github.com/BilkentCompGen/tardis, and a corresponding Docker image is available at https://hub.docker.com/r/alkanlab/tardis/

Contact: fhormozd@ucdavis.edu and calkan@cs.bilkent.edu.tr

1 Introduction

Genomic differences between individuals of the same species, or among different species, range from single nucleotide variation (SNVs) [22] to small insertion/deletions (indels) [26] up to 50 bp, structural variation (SVs) [2] that affect >50 bp, and larger chromosomal aberrations [28]. Among these types of variants, SNVs were extensively and systematically studied since the introduction of microarrays, which can also be used to genotype short indels [22]. SVs, especially copy number variations (CNVs), were first identified using BAC arrays [33, 31], and then oligonucleotide array comparative genomic hybridization [34, 9] and SNV microarrays by analyzing allele frequencies[23, 10]. Chromosomal aberrations such as trisomy, or large translocations (e.g., Philadelphia chromosome [32]) can be tested using fluorescent in-situ hybridization [28].

Fine scale SV discovery was made possible using fosmid-end sequencing [44], and later indels were identified at breakpoint level using whole genome shotgun (WGS) sequencing data [26]. However, both approaches used the Sanger sequencing technology, which is prohibitively expensive to scale to analyze thousands of genomes. High throughput sequencing arose as a cost effective alternative [35] to characterize SVs first using the Roche/454 platform [18], and then Illumina [3, 12, 45, 25, 20, 36, 1, 45].

The 1000 Genomes Project, launched in 2008, used the HTS platforms to catalog SNVs, indels, and SVs in the genomes of 2,504 human individuals [41]. Many algorithms were developed that use one of four basic sequence signatures to discover SVs, namely read depth, read pair, split reads, and assembly [24, 2], however, most of these tools focus on characterizing only a few types of SVs. More modern SV callers such as DELLY [30], LUMPY [19], SV-Bay [17], TIDDIT [11], and TARDIS [37] integrate multiple sequencing signatures to identify a broader range of SVs such as deletions, novel insertions, inversions, and mobile element insertions. However, there is still a need for accurate algorithms to characterize several forms of complex SVs, such as tandem or interspersed segmental duplications (SDs) [8, 7]. Note that read depth based methods can identify the *existence* of SDs [3, 39], but cannot detect the location of the new copies of the duplications. Only SV-Bay [17] and TIDDIT [11] are capable of reporting duplication insertion location using read pair information.

Here we describe novel algorithms to accurately characterize both tandem and interspersed SDs using short read HTS data. Our algorithms make use of multiple sequence signatures to find approximate locations for the duplication insertion breakpoints. We integrated our methods into the TARDIS tool [37] therefore extending its capability to simultaneously detect various types of SVs. We test the new version of TARDIS using both simulated and real data sets. We show that TARDIS achieves 96% sensitivity with only 4% false discovery rate (FDR) in simulation experiments. We also used real WGS data sets generated from two haploid genomes (i.e., CHM1 [15] and CHM13 [38]). Comparison of our predictions with *de novo* assemblies generated using long reads from the same DNA resources [38] revealed ¡5% false discovery rate for the duplications with high score.

The algorithms we describe in this manuscript are among the *first* methods to discover the insertion locations of segmental duplications using high throughput sequencing data. Coupled with the previously documented capability of TARDIS to identify deletions, novel and mobile element insertions, and inversions, we are one more step closer towards a comprehensive characterization of SVs in high throughput sequenced genomes.

2 Methods

2.1 Motivation

The 1000 Genomes Project provides a catalog of SVs in the genomes of 2,504 individuals from many populations [40]. The project primarily focused on characterizing deletions, insertions, and mobile element transpositions, however, it also generated a set of inversion calls. A careful analysis shows that a substantial fraction of the predicted inversions are in fact complex rearrangements that include duplications, inverted duplications, and deletions within an inverted segment (Figure 1). This is because the read pair signatures that signal such complex SVs are exactly the same as shown in Fig. 2. Therefore, any algorithm based on read pair (and/or split read) signature may incorrectly classify these complex events as simple inversions, unless it tries to characterize all such events simultaneously, with additional probabilistic models to differentiate events that show themselves with the same signature.

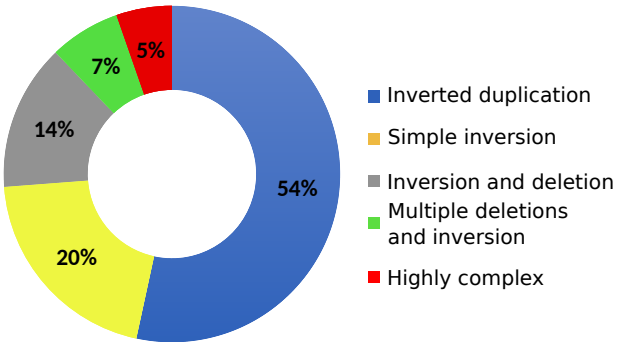

Figure 1: Relative abundance of complex SVs among the inversion calls reported in the 1000 Genomes Project [40]. 54% of predicted inversions are in fact inverted duplications and only 20% are correctly predicted as simple inversions.

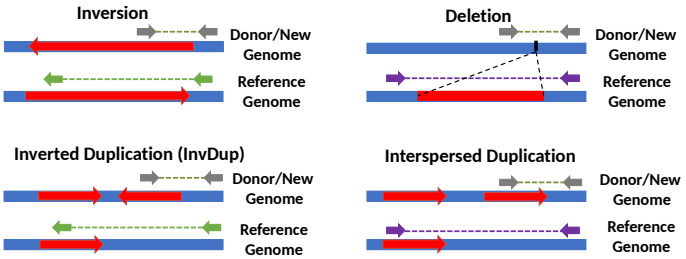

Figure 2: Read pair sequence signatures of inversions, deletions and segmental duplications. The grey arrows show read pairs that span a structural variant breakpoint, and green (left panel) and purple (right panel) arrows show the corresponding map location and orientation of these reads on the reference genome. Note that the read pair signatures for inversions and inverted duplications are exactly the same. Similarly, deletions and direct duplications show the same read pair signature. Therefore read pair based algorithms may incorrectly identify inverted segmental duplications as simple inversions. This problem also exists for incorrectly predicting simple deletions while the true underlying variant is a duplication in direct orientation.

2.2 Read pair and split read clustering

TARDIS uses a combination of read pair, read depth and split read sequencing signatures to discover SVs [37]. TARDIS formulation is based on algorithms we developed earlier using maximum parsimony [12, 14] objective function. The proposed approach has two main steps: First clustering read pairs and split reads that signal each specific type of SV, and second apply a strategy to select a subset of clusters as predicted SV. In this paper we extend TARDIS to characterize a complex set of SVs, which are incorrectly categorized by state of the art methods for SV discovery. Specifically the methods we present here will **advance our capability in discovery of duplication based SVs**. Furthermore, our new methods are capable of separating inversions from more complex events of inverted duplications and are also able to predict the insertion locations of the new copies of segmental duplications. We would argue that considering these more complex types of SV is crucial in improving the accuracy of predicting other types of SVs. We therefore modified TARDIS to calculate a likelihood score for each SV provided the observed read pair, read depth and split read signatures. Figure 3 summarizes the read pair signatures that TARDIS uses to find tandem in direct orientation and interspersed duplications in both direct and inverted orientation. Although not shown on the figure for simplicity, similar rules are required for split reads that signal the same types of SVs (Supplementary Figure 1).

2.2.1 Maximal valid clusters

Our approach for discovery of SVs is based on first produced maximal valid clusters for every type of SVs. We have previously described algorithms to calculate maximal valid clusters for deletions, inversions, and mobile element insertions [12, 13, 14, 37]. A valid cluster is defined as a set of discordant paired-end read alignments that support the same structural variants. In another words, a valid cluster indicates the set of discordant paired-end read mappings that explain the same potential structural variant. More formally, a valid cluster is a set of alignments of discordant read pairs and/or split reads (denoted as rp_i) that support the same particular SV event shown as

$$VClus_i = \{rp_1, rp_2, \ldots, rp_n\}$$

A maximal valid cluster is a valid cluster which no additional discordant paired-end reads can be added to it such that it still remains a valid cluster. Note that, we and others have previously developed methods to efficiently generate all maximal clusters for inversions, deletions, and insertions. In this section we provide new methods to find maximum valid clusters for tandem and interspersed (both direct and inverted) duplications.

There are a set of rules that each rp_i should satisfy in order to support the cluster, $VClus_i$, based on the type of SV.

Inverted duplications : We assume the fragment sizes for read pairs are in the range $[\delta_{min}, \delta_{max}]$, and we denote the insertion breakpoint of the duplication as P_{Br} and the locus of the duplicated sequence is $[P_L, P_R]$ (Figure 3A). We scan the genome from beginning to end, and we consider each position as a potential duplication insertion breakpoint P_{Br}. We consider all sets of read pairs where both mates map to the same strand (i.e., $+/+$ and $-/-$) within interval $[P_{Br} - \delta_{max}, P_{Br}]$ and $[P_{Br}, P_{Br} + \delta_{max}]$ respectively as clusters that potentially signal an inverted duplication.

Interspersed direct duplications : We create the valid clusters in a way similar to the inverted duplications, with the exception of the required read mapping properties. For direct duplications we require

A

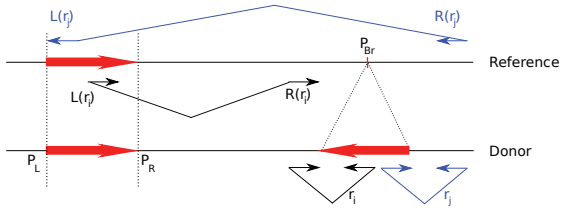

$$\delta_{min} < P_{Br} - R(r_i) + P_R - L(r_i) < \delta_{max}$$

$$\delta_{min} < R(r_j) - P_{Br} + L(r_j) - P_L < \delta_{max}$$

B

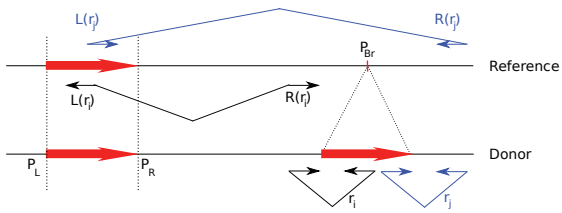

$$\delta_{min} < P_{Br} - R(r_i) + L(r_i) - L(r_i) < \delta_{max}$$

$$\delta_{min} < R(r_j) - P_{Br} + P_R - L(r_j) < \delta_{max}$$

C

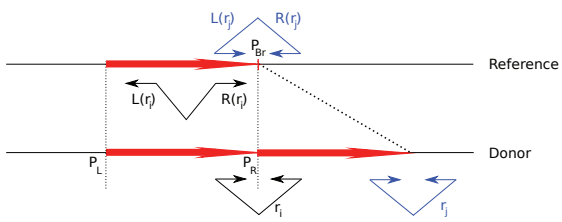

$$\delta_{min} < L(r_i) - P_L + P_R - R(r_i) < \delta_{max}$$

Figure 3: Read pair sequence signatures used in TARDIS to characterize A) interspersed duplications in inverted orientation, B) interspersed duplications in direct orientation, and C) tandem duplications. P_{Br} denotes the breakpoint location of each variant, and P_L and P_R are the left and right (i.e., proximal and distal) coordinates of the duplicated segment. For each type of structural variation, we show two read pairs from the donor genome (r_i, r_j). The read pairs are colored black and blue to facilitate easier tracking by the reader. The alignments for read pair r_i are shown on the reference as $L(r_i)$ and $R(r_i)$, which denote the left (i.e., proximal) and right (i.e., distal) mapping locations of the end reads. Finally, δ_{min} and δ_{max} are the minimum and maximum fragment lengths as inferred from the fragment size distribution in the aligned data.

each mate of a read pair to map to opposing strands (i.e., $+/-$ and $-/+$).

Tandem duplications : We also create the clusters for tandem duplications as shown in Figure 3. In the case of tandem duplications, discordant read pairs and split reads map in opposing strands, where the read mapping to the upstream location will map to the reverse strand, and the read mapping to downstream will map to the forward strand (i.e., $-/+$).

Similar to the valid cluster formulation, a maximal valid cluster is a valid cluster that encompasses all

the valid read pairs and split reads for the particular SV event (i.e., no valid superset exists). This can be computed in polynomial time as follows:

1. We initially create maximal sets $S = \{S_1, S_2, ..., S_k\}$ that harbors the read pair/split read alignments $S_i = \{rp_1, rp_2, ..., rp_k\}$.

2. For interspersed duplications, we use an additional step to bring mappings in both forward-reverse and reverse-forward (forward-forward and reverse-reverse for inverted duplications) orientations together inside the same set.

3. For each maximal overlapping set S_i found in step 1, we create all the overlapping maximal subsets s_i. (This step is necessary only for detecting inversions and interspersed duplications)

4. Among all the sets s_i found in Step 3, remove any set that is a proper subset of another chosen set.

2.3 Probabilistic Model

As we describe above different types of SVs may generate similar discordant read pair signatures (Figure 2). We therefore developed a probabilistic model that makes use of the read depth signature to assign a likelihood score to each potential SV. Our new probabilistic model has the ability to distinguish different types of SVs with the same read pair signature.

2.3.1 Likelihood model

Assume the set of maximum valid clusters $SV = \{S_1, S_2, \ldots, S_n\}$ is observed in the sequenced sample. TARDIS keeps track the following information for each maximum valid cluster S_i for $1 \leq i \leq n$:

- observed read depth and read pair information (d_i, p_i), i.e. d_i is the total observed read depth, and p_i is the number of discordantly mapped read pairs.
- potential duplicated or deleted or inverted region (α_i, β_i).
- potential breakpoint γ_i.
- potential SV type.

Assuming observed read depth and number of discordant read pairs follow a Poisson distribution, $\lambda > 0$,

$$\text{Poisson}(\lambda, x) = \frac{\lambda^x e^{-\lambda}}{x!}$$

here, λ is the expected number of read depth or read pairs, and x is the observed number of read depth or read pairs respectively. However, the expected read depth or read pairs for some events might be zero, we approximate the probability by,

$$\text{Poisson}(0, x) \approx \text{Poisson}(\varepsilon, x)$$

for a small $\varepsilon > 0$ (e.g. $\varepsilon = 0.01$ for read depth and $\varepsilon = 0.001$ for read pairs).

For each cluster S_i, we define a random variable $state_i \in \{0, 1, 2\}$ in which the state of S_i is *homozygous* if $state_i = 2$, *heterozygous* if $state_i = 1$, and *no event* if $state_i = 0$. We also define a random variable $type_i$,

which represents the SV type for S_i. Given $state_i = k$ and $type_i = \delta$, the likelihood of S_i can be calculated as:

$$
\begin{aligned}
L_i(\delta, k) &= P(S_i \mid \delta, k) \\
&= P(\textit{ read depth of } S_i \mid \delta, k) \cdot P(\textit{ read pairs of } S_i \mid \delta, k) \\
&= \text{Poisson}(d_i, \lambda_d) \cdot \text{Poisson}(p_i, \lambda_p) \\
&= \frac{\lambda_d^{d_i} e^{-\lambda_d}}{d_i!} \cdot \frac{\lambda_p^{p_i} e^{-\lambda_p}}{p_i!}
\end{aligned}
$$

where λ_d is the expected read depth of S_i given $type_i = \delta, state_i = k$ and λ_p is the expected read pairs of S_i given $type_i = \delta, state_i = k$.

We calculate λ_d based on $(type_i, state_i)$ and the expected read depth within the region (α_i, β_i) normalized with respect to its G+C content using a sliding window of size 100 bp, denoted by $E_d[(\alpha_i, \beta_i)]$. We calculate λ_p based on the $(type_i, state_i)$ and the expected number of discordantly mapped read pairs around the potential breakpoint γ_i, denoted by $E_p[\gamma_i]$. For instance, if an event is categorized as homozygous deletion, we expect to see almost no read depth inside the potential deleted region (α_i, β_i), and the expected number of discordantly mapped read pairs should be approximately the expected number of reads containing the potential breakpoint, i.e $E_p[\gamma_j]$. For heterozygous deletion events, we expect to see half of the number of read depths and half of the expected number of discordantly mapped read pairs. We also calculate the likelihood score of no event at the potential region given that is categorized as deletion. For this case, we expect to see the expected number of read depths in that potential region and zero discordantly mapped read pairs. Similarly, the value for λ_d, λ_p can be approximately for inversion and duplications. Table 1 shows the value for λ_d, λ_p for each $(type_i, state_i)$ using $E_d[(\alpha_i, \beta_i)]$ and $E_p[\gamma_i]$. Note that even though the formulation for λ_d, λ_p are the same for all types of duplications, the likelihood score will be different because the potential regions (α_i, β_i) are different based on the categorized type of the event being considered. Furthermore, the read-pair support and signature will be different for each type of duplication which is the key in resolving the type of duplication.

Table 1: Formulation for λ_d and λ_p for maximum valid cluster S_i

SV Type	State	λ_d	λ_p
Deletion	*homozygous*	0.01	$E_p[\gamma_i]$
	heterozygous	$0.5 \cdot E_d[(\alpha_i, \beta_i)]$	$0.5 \cdot E_p[\gamma_i]$
	no event	$E_d[(\alpha_i, \beta_i)]$	0.001
Inversion	*homozygous*	$E_d[(\alpha_i, \beta_i)]$	$E_p[\gamma_i]$
	heterozygous	$E_d[(\alpha_i, \beta_i)]$	$0.5 \cdot E_p[\gamma_i]$
	no event	$E_d[(\alpha_i, \beta_i)]$	0.001
Inverted Duplication	*homozygous*	$2 \cdot E_d[(\alpha_i, \beta_i)]$	$E_p[\gamma_i]$
	heterozygous	$1.5 \cdot E_d[(\alpha_i, \beta_i)]$	$0.5 \cdot E_p[\gamma_i]$
	no event	$E_d[(\alpha_i, \beta_i)]$	0.001
Direct Duplication	*homozygous*	$2 \cdot E_d[(\alpha_i, \beta_i)]$	$E_p[\gamma_i]$
	heterozygous	$1.5 \cdot E_d[(\alpha_i, \beta_i)]$	$0.5 \cdot E_p[\gamma_i]$
	no event	$E_d[(\alpha_i, \beta_i)]$	0.001
Tandem Duplication	*homozygous*	$2 \cdot E_d[(\alpha_i, \beta_i)]$	$E_p[\gamma_i]$
	heterozygous	$1.5 \cdot E_d[(\alpha_i, \beta_i)]$	$0.5 \cdot E_p[\gamma_i]$
	no event	$E_d[(\alpha_i, \beta_i)]$	0.001

2.3.2 SV weight

For each potential SV we calculate a score to represent how likely a SV prediction is correct given the observed signature. Note that, for each SV, we calculate the likelihood considering homozygous state and heterozygous state separately.

We define the score as ratio of log of likelihoods of the putative SV being true given the observed data over it being false. Note that we use log function to avoid numerical errors. Even those the standard approach is to use logarithm of the ratio, we heuristically use the ratio to make sure that the scores are positive, which will work better for the set cover approximation algorithm we will use in the next step.

The score of potential SV S_i is defined as follows:

$$score(S_i) = \frac{\max\left(\log L_i(\delta_i, k=1), \log L_i(\delta_i, k=2)\right)}{\log L_i(\delta_i, k=0)}$$

where δ_i is the potential SV type of S_i. Again, $k = 0, 1, 2$ implies that the state of S_i is *no event*, *heterozygous*, *homozygous* respectively.

2.3.3 Multi-mapping reads

We have previously showed that a greedy approach motivated by weighted-set cover problem performs well in discovery of SVs with multiple mapping of the reads [12]. It guaranties an $O(\log(n))$ approximation. We therefore utilize a similar iterative greedy approach here as minimum weighted-set cover. More formally, at each step we select the set with the lowest ratio of SV score ($score(S_i)$) and number of uncovered discordant paired end-reads being covered by that SV (p_i)

$$weight(S_i) = \frac{score(S_i)}{p_i}$$

and continues this iterative process.

3 Results

3.1 Simulation

In order to evaluate performance of our SV detection algorithms, we generated a simulated genome first using VarSim [27]. VarSim "inserts" previously known real genomic variants into a given reference segment. Although it supports deletions, inversions, and tandem duplications, it does not yet simulate interspersed segmental duplications. Therefore we developed a new simulator called CNVSim to additionally simulate interspersed duplications in both direct and inverted duplication.

In total, we simulated SVs of lengths selected uniformly random between 500 bp and 10 Kbp. For inverted duplications and interspersed direct duplications, the distance from the new paralog to the original copy is chosen uniformly random between 5,000 bp and 50 Kbp. All segments are sampled randomly from the well-defined (i.e., no assembly gaps) regions in the reference genome, and guaranteed to be non-overlapping. Each simulated SV can be in homozygous or heterozygous state.

Based on the human reference genome (GRCh37), we simulated total of 1,200 SVs including 700 deletions, 579 inversions, 200 tandem duplications, 200 inverted duplications, and 200 interspersed direct duplications. We then simulated WGS data at four depth of coverages 10×, 20×, 30×, 60× using wgsim (https://github.com/lh3/wgsim). We mapped the reads back to the human reference genome (GRCh37)

using BWA-MEM [21]. Finally we obtained structural variation call sets using TARDIS, DELLY [30], LUMPY [19], TIDDIT [11], and SoftSV [4].

We included analysis of all types of SVs in our simulation and real data experiments following our motivation we outlined in section 2.1 and Figures 1 and 2. We would like to reiterate that inability to call interspersed segmental duplications results in higher false positives in both deletion and inversion discovery. Through characterization of segmental duplications and integration of a read depth based probabilistic model, TARDIS achieves better inversion and deletion discovery accuracy by correct classification of more complex SV types. Further analysis on the simulations revealed that 95 of 773 deletions predicted by LUMPY and 96 of 852 deletions predicted by DELLY are indeed interspersed duplications in direct orientation. Similarly, 109 of 1,286 DELLY-predicted inversions were in fact inverted segmental duplications.

Finally, we simulated 10 large (up to 1 Mbp) segmental duplications in chromosome Y to assess the power of TARDIS in detecting large duplications. TARDIS correctly identified 4/10 duplications of size >63 Kb (Supplementary Table S1).

Table 2: Summary of simulation predictions by TARDIS, TIDDIT, LUMPY, SoftSV and DELLY.

SV Type	Cov.	TARDIS			TIDDIT			LUMPY			SoftSV			DELLY		
		MISS	FDR	TPR	MISS	FDR	TPR	MISS	FDR	TPR	MISS	FDR	TPR	MISS	FDR	TPR
Deletion	10×	244	**0.00**	0.65	288	**0.00**	0.59	205	0.26	**0.71**	272	0.30	0.61	255	0.28	0.64
	20×	113	**0.00**	**0.84**	226	**0.00**	0.68	125	0.25	0.82	135	0.32	0.81	124	0.27	0.82
	30×	92	**0.00**	**0.87**	194	**0.00**	0.72	111	0.24	0.84	109	0.32	0.84	106	0.30	0.85
	60×	76	0.01	**0.89**	185	**0.00**	0.74	96	0.24	0.86	97	0.33	0.86	99	0.31	0.86
Inversion	10×	108	0.03	**0.81**	119	0.45	0.79	121	**0.00**	0.79	121	**0.00**	0.79	140	0.41	0.76
	20×	98	0.06	0.83	97	0.44	0.83	102	**0.01**	0.82	77	0.03	**0.87**	94	0.41	0.84
	30×	88	0.06	0.85	101	0.44	0.83	98	**0.01**	0.83	65	0.03	**0.89**	87	0.43	0.85
	60×	83	0.06	0.86	96	0.44	0.83	93	**0.01**	0.84	78	0.05	**0.87**	84	0.43	0.85
Duplication	10×	72	**0.05**	**0.88**	428	0.10	0.29	428	0.49	0.29	444	0.55	0.26	433	0.48	0.28
	20×	28	**0.05**	**0.95**	422	0.09	0.30	412	0.50	0.31	410	0.55	0.32	429	0.50	0.29
	30×	25	**0.04**	**0.96**	424	0.10	0.29	410	0.50	0.32	403	0.57	0.33	419	0.50	0.30
	60×	19	0.09	**0.97**	422	**0.08**	0.30	408	0.50	0.32	401	0.60	0.33	414	0.50	0.31

We show the true positive rate/recall and false discovery rates (TPR and FDR) of TARDIS, TIDDIT, LUMPY, SoftSV and DELLY at different depths of coverage from 10× to 60× for deletions (Del), inversions (Inv), and segmental duplications (Dup). Note that only TARDIS can predict interspersed segmental duplications, therefore other tools miss such events. TARDIS consistently shows low FDR with comparable sensitivity. In our simulation, the length of each SV is generated uniformly random between 500 bp and 10 Kbp. Note that the bold values for FDR and TPR represent the best results among the five tools.

Table 2 shows the true positive rate (TPR) and false discovery rate (FDR) of TARDIS compared to DELLY, LUMPY, TIDDIT and SoftSV on the simulated data. TARDIS achieved a substantially higher TPR and a lower FDR for deletions and duplications overall. Additionally, its sensitivity is comparable to LUMPY and SoftSV in terms of inversion predictions. (See Supplementary Figure 2 for precision-recall curves of inversions and duplications.)

In these simulation experiments we used the default variables, which require at least 5 read pairs that support the SV event. Although this cut off works well, it contributes to higher number of false positives when the depth of coverage is high (Table 2). To demonstrate the effects of the values for this parameter, we repeated the experiment with varying minimum number of read pair support values. We confirmed that with higher values, we can reduce the FDR for high coverage genomes (Supplementary Table S2).

Furthermore, TARDIS can classify duplications into tandem, interspersed directed duplication and inverted duplication. However, DELLY, LUMPY, TIDDIT and SoftSV are not designed to characterize interspersed segmental duplications, therefore we cannot provide comparisons. Table 3 shows the TDR, FDR, and the exact count of the number of True/False predictions for each type of segmental duplication.

Table 3: Characterization of different types of segmental duplications using TARDIS on simulated data.

Duplication Type	Coverage	# SVs	Missed	True	TPR	False	FDR
Inverted Interspersed Duplication	10×	200	15	185	0.93	7	0.04
	20×	200	10	190	0.95	11	0.05
	30×	200	12	188	0.94	15	0.07
	60×	200	9	191	0.96	33	0.15
Direct Interspersed Duplication	10×	200	10	190	0.95	3	0.02
	20×	200	7	193	0.97	0	0.00
	30×	200	6	194	0.97	4	0.02
	60×	200	5	195	0.98	9	0.04
Tandem Duplication	10×	200	47	153	0.77	21	0.12
	20×	200	11	189	0.95	15	0.07
	30×	200	7	193	0.97	10	0.05
	60×	200	5	195	0.98	16	0.08

TARDIS can classify duplications into tandem, interspersed directed duplication and inverted duplication. However, DELLY, LUMPY, TIDDIT and SoftSV are not designed to characterize these complex SVs. This table shows the true positive rate (recall) and false discovery rate (TPR and FDR respectively) of TARDIS for each type of duplication.

3.2 Haploid genome analyses

As the first experiment with real data sets, we downloaded short read HTS data generated from two haploid cell lines, namely CHM1 and CHM13 [16, 38]. We mapped the reads to human reference genome (GRCh37) using BWA-MEM [21]. We also obtained call sets generated with PacBio data from the same genomes [6], but here we use updated SV calls (Mark Chaisson, personal communication), which we use as the true inversion set to compare with our predictions.

We present the comparison of the inversion predictions made by TARDIS and two state of the art methods LUMPY and DELLY in Figure 4. Note that we only consider inversions of length > 100 bp. Figure 4) (a) & (b) show the comparison of TARDIS predictions with those of other tools on CHM1 and CHM13 respectively (We also present a similar comparison for deletion predictions in Supplementary Figure 3). Overall, TARDIS achieves better accuracy. We also tested the highest scoring set (n=50) of predicted inversions by each tool generated for the CHM1 genome. Briefly, we used a reference-guided *de novo* assembly of PacBio reads generated from the same genome [6] and mapped the contigs to the loci of interest. We show a receiver-operating-charasteristic-like plot that uses actual numbers of true and false calls instead of rates (TPR/FDR) (Supplementary Figure 4). Here we observe that compared to LUMPY and DELLY, TARDIS achieves better area under the curve. However, we note that the main reason for DELLY and LUMPY curves being closer to that of TARDIS for low number of false calls is because there were several predictions for which corresponding contigs did not exist in the assembled genome, therefore omitted from this plot.

We provide the full set of the 50 highest scoring segmental duplications that TARDIS predicts in the CHM1 genome together with *in silico* validation using the corresponding PacBio-based assembly (Table 4). Almost all of the predicted duplications, except one, were validated using long reads. We provide the PacBio alignments of some of these events and top 20 highest scoring CHM13 predictions in Supplementary Materials. Note that in most cases TARDIS assigned the correct subtype of duplications (inverted, direct or tandem duplication) to the prediction. As expected, the highest number of segmental duplications in the top 50 were tandem duplications ($> 50\%$ of all duplications).

Table 4: 50 highest scoring segmental duplications predicted by TARDIS in the CHM1 genome.

Duplication Insertion Locus				TARDIS Dup. Type	TARDIS Score	Validation (PacBio)	Duplication Insertion Locus				TARDIS Dup. Type	TARDIS Score	Validation (PacBio)
chr11	63,701,552	-	63,702,044	Direct	0.000096	True	chr2	37,928,294	-	38,101,823	Tandem	0.000073	N/A
chr3	194,546,158	-	194,546,552	Direct	0.000100	True	chr20	60,032,848	-	60,033,403	Tandem	0.000080	True
chr5	143,512,369	-	143,512,967	Direct	0.000139	True	chr5	3,323,855	-	3,324,309	Tandem	0.000106	N/A
chr2	240,640,651	-	240,641,122	Direct	0.000199	True	chr7	2,554,464	-	2,554,791	Tandem	0.000111	True
chr20	2,359,605	-	2,360,003	Direct	0.000271	True	chr12	110,099,340	-	110,099,746	Tandem	0.000117	True
chr9	112,285,747	-	112,286,145	Direct	0.000300	True	chr6	168,052,194	-	168,052,468	Tandem	0.000117	True
chr8	2,215,143	-	2,215,392	Direct	0.000310	N/A	chr1	207,097,489	-	207,097,910	Tandem	0.000123	True
chr18	69,711,702	-	69,712,115	Direct	0.000323	True	chr16	86,008,734	-	86,009,147	Tandem	0.000127	True
chr17	46,615,512	-	46,615,903	Direct	0.000326	True	chr17	80,317,607	-	80,318,019	Tandem	0.000127	N/A
chr6	160,877,582	-	160,878,047	Direct	0.000342	N/A	chr10	127,513,435	-	127,513,672	Tandem	0.000129	True
chr2	125,052,915	-	125,053,261	Inverted	0.000088	True	chr14	106,049,125	-	106,049,349	Tandem	0.000129	True
chr3	43,834,996	-	43,835,748	Inverted	0.000089	True	chr6	44,012,338	-	44,012,957	Tandem	0.000129	True
chr14	67,171,710	-	67,172,020	Inverted	0.000092	True	chr9	132,158,817	-	132,159,088	Tandem	0.000129	N/A
chr2	72,440,071	-	72,440,597	Inverted	0.000105	True	chr12	13,164,470	-	13,164,800	Tandem	0.000136	True
chr9	107,816,537	-	107,817,079	Inverted	0.000140	True	chr20	62,720,020	-	62,720,215	Tandem	0.000136	True
chr17	36,405,748	-	36,407,397	Inverted	0.000149	False	chr10	132,974,754	-	132,975,320	Tandem	0.000144	True
chr1	114,645,858	-	114,646,155	Inverted	0.000235	True	chr8	2,215,817	-	2,216,236	Tandem	0.000144	N/A
chr5	115,350,905	-	115,351,086	Inverted	0.000236	True	chr9	34,681,581	-	34,681,899	Tandem	0.000194	True
chr12	71,532,699	-	71,533,378	Inverted	0.000245	True	chr6	35,754,661	-	35,766,731	Tandem	0.000255	True
chr7	31,586,861	-	31,587,129	Inverted	0.000278	True	chr20	62,123,612	-	62,124,210	Tandem	0.000257	True
chr18	11,511,287	-	11,511,480	Inverted	0.000280	True	chr20	59,567,884	-	59,590,251	Tandem	0.000268	True
							chr18	77,831,329	-	77,831,784	Tandem	0.000273	N/A
							chrX	417,958	-	418,361	Tandem	0.000273	True
							chr20	42,325,214	-	42,325,573	Tandem	0.000290	True
							chr19	34,882,471	-	34,883,258	Tandem	0.000310	True
							chr2	3,184,299	-	3,185,046	Tandem	0.000310	N/A
							chr3	197,117,159	-	197,117,807	Tandem	0.000318	N/A

Here we list the insertion locations of the top 50 scoring segmental duplications in CHM1 genome. All predictions are sorted by the SV score (lower is better). If the validation is N/A, that means the incorrect prediction from PacBio data, which will be skipped in the comparison. TARDIS only gives one false call and three interspersed duplications that are wrongly assigned to tandem duplications.

3.3 NA12878 genome

We also analyzed the WGS data generated from NA12878 using TARDIS for various types of SV discovery and compared the results against state-of-the-art methods for inversion prediction. Similar to the simulation and CHM1/13 results, TARDIS outperformed the tested methods for SV discovery (see Supplementary Figure 16 for inversion comparison with a set of validated inversions on this sample).

More interestingly, we have found an example of a large inverted duplication in NA12878 sample which we validated using available orthogonal PacBio data generated from the same sample (Figure 5). The interesting point about this inverted duplication is that it is larger than 10 Kbp and the distance between locus of insertion and the duplicated region is also larger, which shows a potential start of a new segmental duplication.

4 Discussion

Characterization of structural variants using HTS data is a well-studied problem. Still, due to the difficulty of accurately predicting complex variants, most of the current approaches mainly focus on specific forms of SVs. In this paper we describe novel algorithms to detect complex SV events such as tandem, direct and inverted interspersed segmental duplications simultaneously with simpler forms SV using whole genome sequencing data. Our approach integrates multiple sequence signatures to identify and cluster potential SV regions under the assumption of maximum parsimony. However, complex SV events usually generate

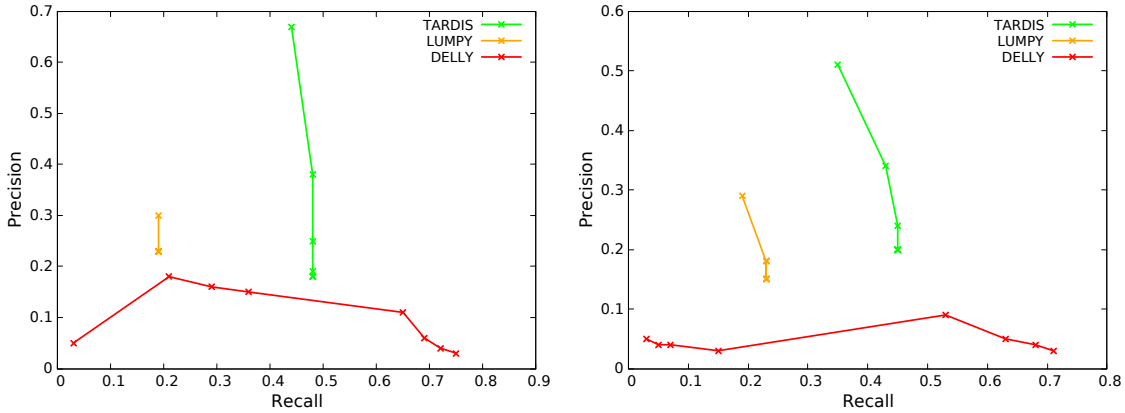

(a) Precision-recall curves for CHM1

(b) Precision-recall curves for CHM13

Figure 4: Precision - Recall curves for the comparison of inversion predictions on CHM1 and CHM13 genomes. Overall TARDIS achieves better accuracy than the two other approaches tested. (a), (b) comparison of CHM1 and CHM13 predicted inversions using PacBio reads based on BLASR mappings.

similar signatures (i.e., inversion vs. inverted duplication), which make it difficult to differentiate particular SV types. Therefore, we strengthened our method by using a probabilistic likelihood model to overcome this obstacle by calculating a likelihood score for each SV.

Using simulated and real data sets, we showed that TARDIS outperforms state-of-the art methods in terms of specificity for all types of SVs, and achieves considerably high true discovery rate for segmental duplications with moderate time and memory requirements (See Supplementary Table S4 for a comparison of different tools for CHM1 and NA12878 genomes.). It should be noted that it TARDIS is currently one of the few methods that can classify duplications as tandem and interspersed in direct or inverted orientation using HTS data. Additionally, it demonstrates comparable sensitivity in deletions and inversions.

Here we only focused on tandem duplications in direct orientation, although inverted tandem repeats in genomes, or DNA palindromes, also exist especially in the human Y chromosome [5, 43]. However, these DNA palindromes were incorporated in the human genome over millions of years of evolution, and polymorphic inverted tandem duplication events are rare. Because of this, the mechanisms forming DNA palindromes are not yet well-established and we are not aware of a resource of validated DNA palindrome polymorphisms. We therefore ignore such variants in this study and we aim to address them in the future.

Future improvements in TARDIS will include addition of local assembly signature to help it achieve better accuracy. Although simulation experiments demonstrated potential efficacy of TARDIS in segmental duplication predictions, those that are generated from real genomes need to be experimentally verified to fully understand the power and shortcomings of the TARDIS algorithm. We can then apply TARDIS to thousands of genomes that were already sequenced as part of various projects, such as the 1000 Genomes Project to advance our understanding of the SV spectrum in human genomes. Another possible direction for TARDIS can be integration of new methods to better detect somatic structural variation detection, which we can then apply to cancer genomes.

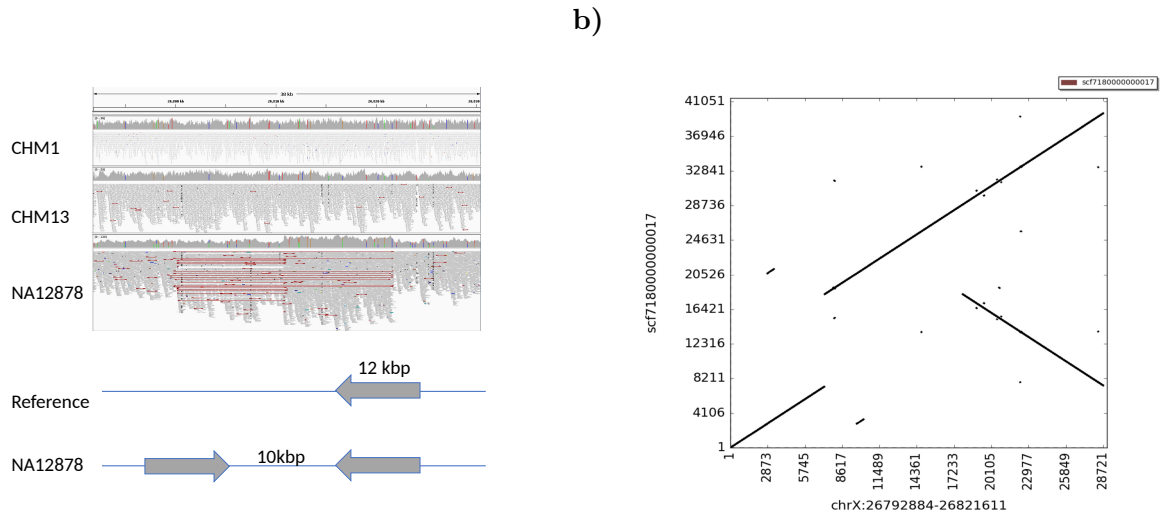

Figure 5: a) Illumina read mapping information visualized using IGV[42]. Here the read pairs in the NA12878 genome show typical inversion signature (red lines), where all reads map concordantly in CHM1 and CHM13 genomes, and a simple sketch of the alternative inverted duplication structure of the same region. b) Dot plot matrix validation using PacBio data, which shows an inverted duplication. The whole genome assembly shows an inverted duplication of a 12 Kb segment separated by 10 Kb. This region demonstrates the case where read pair based clustering confuses an inverted duplication with a simple inversion.

Acknowledgements

We thank E. Ebren and F. Karaoglanoglu for their help in creating simulation data sets. We would thank Evan E. Eichler for insightful advise and comments. Part of the work was done during FH postdoc training in Evan E. Eichler's lab. We would also like to Mark Chaisson for providing PacBio call sets for CHM1 and CHM13, and the local assembly of these genomes.

Funding

This work was supported by a grant by a TÜBİTAK (215E172), and an EMBO Installation Grant (IG-2521) to C.A., and an NSF grant (1528234) to F.H. The authors also acknowledge the Computational Genomics Summer Institute funded by NIH grant GM112625 that fostered international collaboration among the groups involved in this project.

Availability

TARDIS is available under BSD 3-clause license at `https://github.com/BilkentCompGen/tardis`, and the CNVSim simulator is available at `https://github.com/LeMinhThong/CNVSim`. NA12878 WGS data set can be downloaded from `https://www.illumina.com/platinumgenomes.html`. SRA IDs for CHM1 and CHM13 are SRP044331 and SRP080317, respectively. GenBank assembly accession numbers for CHM1 and CHM13 assemblies are GCA_000306695.2 and GCA_000983455.2.

References

[1] Alexej Abyzov, Alexander E. Urban, Michael Snyder, and Mark Gerstein. CNVnator: an approach to discover, genotype, and characterize typical and atypical CNVs from family and population genome sequencing. *Genome Res*, 21(6):974–984, Jun 2011.

[2] Can Alkan, Bradley P Coe, and Evan E Eichler. Genome structural variation discovery and genotyping. *Nat Rev Genet*, 12(5):363–376, May 2011.

[3] Can Alkan, Jeffrey M Kidd, Tomas Marques-Bonet, Gozde Aksay, Francesca Antonacci, Fereydoun Hormozdiari, Jacob O Kitzman, Carl Baker, Maika Malig, Onur Mutlu, S. Cenk Sahinalp, Richard A Gibbs, and Evan E Eichler. Personalized copy number and segmental duplication maps using next-generation sequencing. *Nat Genet*, 41(10):1061–1067, Oct 2009.

[4] Christoph Bartenhagen and Martin Dugas. Robust and exact structural variation detection with paired-end and soft-clipped alignments: SoftSV compared with eight algorithms. *Briefings in Bioinformatics*, 17:51–62, January 2016.

[5] Harrison Brand, Ryan L Collins, Carrie Hanscom, Jill A Rosenfeld, Vamsee Pillalamarri, Matthew R Stone, Fontina Kelley, Tamara Mason, Lauren Margolin, Stacey Eggert, Elyse Mitchell, Jennelle C Hodge, James F Gusella, Stephan J Sanders, and Michael E Talkowski. Paired-duplication signatures mark cryptic inversions and other complex structural variation. *American journal of human genetics*, 97:170–176, July 2015.

[6] Mark J P. Chaisson, John Huddleston, Megan Y. Dennis, Peter H. Sudmant, Maika Malig, Fereydoun Hormozdiari, Francesca Antonacci, Urvashi Surti, Richard Sandstrom, Matthew Boitano, Jane M. Landolin, John A. Stamatoyannopoulos, Michael W. Hunkapiller, Jonas Korlach, and Evan E. Eichler. Resolving the complexity of the human genome using single-molecule sequencing. *Nature*, 517:608–611, Jan 2015.

[7] Mark J.P. Chaisson, Ashley D. Sanders, Xuefang Zhao, Ankit Malhotra, David Porubsky, Tobias Rausch, Eugene J. Gardner, Oscar Rodriguez, Li Guo, Ryan L. Collins, Xian Fan, Jia Wen, Robert E. Handsaker, Susan Fairley, Zev N. Kronenberg, Xiangmeng Kong, Fereydoun Hormozdiari, Dillon Lee, Aaron M. Wenger, Alex Hastie, Danny Antaki, Peter Audano, Harrison Brand, Stuart Cantsilieris, Han Cao, Eliza Cerveira, Chong Chen, Xintong Chen, Chen-Shan Chin, Zechen Chong, Nelson T. Chuang, Deanna M. Church, Laura Clarke, Andrew Farrell, Joey Flores, Timur Galeev, Gorkin David, Madhusudan Gujral, Victor Guryev, William Haynes-Heaton, Jonas Korlach, Sushant Kumar, Jee Young Kwon, Jong Eun Lee, Joyce Lee, Wan-Ping Lee, Sau Peng Lee, Patrick Marks, Karine Valud-Martinez, Sascha Meiers, Katherine M. Munson, Fabio Navarro, Bradley J. Nelson, Conor Nodzak, Amina Noor, Sofia Kyriazopoulou-Panagiotopoulou, Andy Pang, Yunjiang Qiu, Gabriel Rosanio, Mallory Ryan, Adrian Stutz, Diana C.J. Spierings, Alistair Ward, AnneMarie E. Welsch, Ming Xiao, Wei Xu, Chengsheng Zhang, Qihui Zhu, Xiangqun Zheng-Bradley, Goo Jun, Li Ding, Chong Lek Koh, Bing Ren, Paul Flicek, Ken Chen, Mark B. Gerstein, Pui-Yan Kwok, Peter M. Lansdorp, Gabor Marth, Jonathan Sebat, Xinghua Shi, Ali Bashir, Kai Ye, Scott E. Devine, Michael Talkowski, Ryan E. Mills, Tobias Marschall, Jan Korbel, Evan E. Eichler, and Charles Lee. Multi-platform discovery of haplotype-resolved structural variation in human genomes. *bioRxiv*, 2017.

[8] M.J.P. Chaisson, R.K. Wilson, and E. E. Eichler. Genetic variation and the de novo assembly of human genomes. *Nature Reviews Genetics*, 16:627–640, November 2015.

[9] Donald F Conrad, Dalila Pinto, Richard Redon, Lars Feuk, Omer Gokcumen, Yujun Zhang, Jan Aerts, T. Daniel Andrews, Chris Barnes, Peter Campbell, Tomas Fitzgerald, Min Hu, Chun Hwa Ihm, Kati Kristiansson, Daniel G Macarthur, Jeffrey R Macdonald, Ifejinelo Onyiah, Andy Wing Chun Pang, Sam Robson, Kathy Stirrups, Armand Valsesia, Klaudia Walter, John Wei, Wellcome Trust Case Control Consortium, Chris Tyler-Smith, Nigel P Carter, Charles Lee, Stephen W Scherer, and Matthew E Hurles. Origins and functional impact of copy number variation in the human genome. *Nature*, 464(7289):704–712, Apr 2010.

[10] Gregory M Cooper, Troy Zerr, Jeffrey M Kidd, Evan E Eichler, and Deborah A Nickerson. Systematic assessment of copy number variant detection via genome-wide SNP genotyping. *Nat Genet*, 40(10):1199–1203, Oct 2008.

[11] Jesper Eisfeldt, Francesco Vezzi, Pall Olason, Daniel Nilsson, and Anna Lindstrand. TIDDIT, an efficient and comprehensive structural variant caller for massive parallel sequencing data. *F1000Research*, 6:664, 2017.

[12] Fereydoun Hormozdiari, Can Alkan, Evan E Eichler, and S. Cenk Sahinalp. Combinatorial algorithms for structural variation detection in high-throughput sequenced genomes. *Genome Res*, 19(7):1270–1278, Jul 2009.

[13] Fereydoun Hormozdiari, Can Alkan, Mario Ventura, Iman Hajirasouliha, Maika Malig, Faraz Hach, Deniz Yorukoglu, Phuong Dao, Marzieh Bakhshi, S. Cenk Sahinalp, and Evan E Eichler. Alu repeat discovery and characterization within human genomes. *Genome Res*, 21(6):840–849, Jun 2011.

[14] Fereydoun Hormozdiari, Iman Hajirasouliha, Andrew McPherson, Evan E Eichler, and S. Cenk Sahinalp. Simultaneous structural variation discovery among multiple paired-end sequenced genomes. *Genome Res*, 21(12):2203–2212, Dec 2011.

[15] John Huddleston, Mark Jp Chaisson, Karyn Meltz Steinberg, Wes Warren, Kendra Hoekzema, David S Gordon, Tina A Graves-Lindsay, Katherine M Munson, Zev N Kronenberg, Laura Vives, Paul Peluso, Matthew Boitano, Chen-Shin Chin, Jonas Korlach, Richard K Wilson, and Evan E Eichler. Discovery and genotyping of structural variation from long-read haploid genome sequence data. *Genome research*, November 2016.

[16] John Huddleston, Swati Ranade, Maika Malig, Francesca Antonacci, Mark Chaisson, Lawrence Hon, Peter H. Sudmant, Tina A. Graves, Can Alkan, Megan Y. Dennis, Richard K. Wilson, Stephen W. Turner, Jonas Korlach, and Evan E. Eichler. Reconstructing complex regions of genomes using long-read sequencing technology. *Genome Res*, 24(4):688–696, Apr 2014.

[17] Daria Iakovishina, Isabelle Janoueix-Lerosey, Emmanuel Barillot, Mireille Regnier, and Valentina Boeva. SV-Bay: structural variant detection in cancer genomes using a Bayesian approach with correction for GC-content and read mappability. *Bioinformatics*, 32:984–992, April 2016.

[18] Jan O Korbel, Alexander Eckehart Urban, Jason P Affourtit, Brian Godwin, Fabian Grubert, Jan Fredrik Simons, Philip M Kim, Dean Palejev, Nicholas J Carriero, Lei Du, Bruce E Taillon, Zhoutao Chen, Andrea Tanzer, A. C Eugenia Saunders, Jianxiang Chi, Fengtang Yang, Nigel P Carter, Matthew E Hurles, Sherman M Weissman, Timothy T Harkins, Mark B Gerstein, Michael Egholm, and Michael Snyder. Paired-end mapping reveals extensive structural variation in the human genome. *Science*, 318(5849):420–426, Oct 2007.

[19] Ryan M. Layer, Colby Chiang, Aaron R. Quinlan, and Ira M. Hall. LUMPY: a probabilistic framework for structural variant discovery. *Genome Biol*, 15(6):R84, 2014.

[20] Seunghak Lee, Fereydoun Hormozdiari, Can Alkan, and Michael Brudno. MoDIL: detecting small indels from clone-end sequencing with mixtures of distributions. *Nat Methods*, 6(7):473–474, Jul 2009.

[21] Heng Li. Aligning sequence reads, clone sequences and assembly contigs with BWA-MEM. *arXiv preprint arXiv:1303.3997*, 2013.

[22] G. T. Marth, I. Korf, M. D. Yandell, R. T. Yeh, Z. Gu, H. Zakeri, N. O. Stitziel, L. Hillier, P. Y. Kwok, and W. R. Gish. A general approach to single-nucleotide polymorphism discovery. *Nat Genet*, 23(4):452–456, Dec 1999.

[23] Steven A. McCarroll, Tracy N. Hadnott, George H. Perry, Pardis C. Sabeti, Michael C. Zody, Jeffrey C. Barrett, Stephanie Dallaire, Stacey B. Gabriel, Charles Lee, Mark J. Daly, David M. Altshuler, and International HapMap Consortium . Common deletion polymorphisms in the human genome. *Nat Genet*, 38(1):86–92, Jan 2006.

[24] Paul Medvedev and Michael Brudno. *Ab Initio Whole Genome Shotgun Assembly with Mated Short Reads*, pp. 50–64. Springer Berlin Heidelberg, Berlin, Heidelberg, 2008.

[25] Paul Medvedev, Monica Stanciu, and Michael Brudno. Computational methods for discovering structural variation with next-generation sequencing. *Nat Methods*, 6(11 Suppl):S13–S20, Nov 2009.

[26] Ryan E Mills, Christopher T Luttig, Christine E Larkins, Adam Beauchamp, Circe Tsui, W. Stephen Pittard, and Scott E Devine. An initial map of insertion and deletion (INDEL) variation in the human genome. *Genome Res*, 16(9):1182–1190, Sep 2006.

[27] John C. Mu, Marghoob Mohiyuddin, Jian Li, Narges Bani Asadi, Mark B. Gerstein, Alexej Abyzov, Wing H. Wong, and Hugo Y K. Lam. VarSim: a high-fidelity simulation and validation framework for high-throughput genome sequencing with cancer applications. *Bioinformatics*, 31(9):1469–1471, May 2015.

[28] G Obe, P Pfeiffer, J R K Savage, C Johannes, W Goedecke, P Jeppesen, A T Natarajan, W Martínez-López, G A Folle, and M E Drets. Chromosomal aberrations: formation, identification and distribution. *Mutation research*, 504:17–36, July 2002.

[29] Matthew Pendleton, Robert Sebra, Andy Wing Chun Pang, Ajay Ummat, Oscar Franzen, Tobias Rausch, Adrian M Stütz, William Stedman, Thomas Anantharaman, Alex Hastie, Heng Dai, Markus Hsi-Yang Fritz, Han Cao, Ariella Cohain, Gintaras Deikus, Russell E Durrett, Scott C Blanchard, Roger Altman, Chen-Shan Chin, Yan Guo, Ellen E Paxinos, Jan O Korbel, Robert B Darnell, W Richard McCombie, Pui-Yan Kwok, Christopher E Mason, Eric E Schadt, and Ali Bashir. Assembly and diploid architecture of an individual human genome via single-molecule technologies. *Nature methods*, 12:780–786, August 2015.

[30] Tobias Rausch, Thomas Zichner, Andreas Schlattl, Adrian M. Stütz, Vladimir Benes, and Jan O. Korbel. DELLY: structural variant discovery by integrated paired-end and split-read analysis. *Bioinformatics*, 28(18):i333–i339, Sep 2012.

[31] Richard Redon, Shumpei Ishikawa, Karen R Fitch, Lars Feuk, George H Perry, T. Daniel Andrews, Heike Fiegler, Michael H Shapero, Andrew R Carson, Wenwei Chen, Eun Kyung Cho, Stephanie Dallaire, Jennifer L Freeman, Juan R González, Mònica Gratacòs, Jing Huang, Dimitrios Kalaitzopoulos, Daisuke Komura, Jeffrey R MacDonald, Christian R Marshall, Rui Mei, Lyndal Montgomery, Kunihiro Nishimura, Kohji Okamura, Fan Shen, Martin J Somerville, Joelle Tchinda, Armand Valsesia, Cara Woodwark, Fengtang Yang, Junjun Zhang, Tatiana Zerjal, Jane Zhang, Lluis Armengol, Donald F Conrad, Xavier Estivill, Chris Tyler-Smith, Nigel P Carter, Hiroyuki Aburatani, Charles Lee, Keith W Jones, Stephen W Scherer, and Matthew E Hurles. Global variation in copy number in the human genome. *Nature*, 444(7118):444–454, Nov 2006.

[32] J D Rowley. Letter: A new consistent chromosomal abnormality in chronic myelogenous leukaemia identified by quinacrine fluorescence and giemsa staining. *Nature*, 243:290–293, June 1973.

[33] Jonathan Sebat, B. Lakshmi, Jennifer Troge, Joan Alexander, Janet Young, Pär Lundin, Susanne Månér, Hillary Massa, Megan Walker, Maoyen Chi, Nicholas Navin, Robert Lucito, John Healy, James Hicks, Kenny Ye, Andrew Reiner, T Conrad Gilliam, Barbara Trask, Nick Patterson, Anders Zetterberg, and Michael Wigler. Large-scale copy number polymorphism in the human genome. *Science*, 305(5683):525–528, Jul 2004.

[34] Andrew J Sharp, Sierra Hansen, Rebecca R Selzer, Ze Cheng, Regina Regan, Jane A Hurst, Helen Stewart, Sue M Price, Edward Blair, Raoul C Hennekam, Carrie A Fitzpatrick, Rick Segraves, Todd A Richmond, Cheryl Guiver, Donna G Albertson, Daniel Pinkel, Peggy S Eis, Stuart Schwartz, Samantha J L Knight, and Evan E Eichler. Discovery of previously unidentified genomic disorders from the duplication architecture of the human genome. *Nat Genet*, 38(9):1038–1042, Sep 2006.

[35] Jay Shendure and Hanlee Ji. Next-generation DNA sequencing. *Nat Biotechnol*, 26(10):1135–1145, Oct 2008.

[36] Suzanne Sindi, Elena Helman, Ali Bashir, and Benjamin J Raphael. A geometric approach for classification and comparison of structural variants. *Bioinformatics*, 25:i222–i230, June 2009.

[37] Arda Soylev, Can Kockan, Fereydoun Hormozdiari, and Can Alkan. Toolkit for automated and rapid discovery of structural variants. *Methods*, 129:3–7, 2017.

[38] Karyn Meltz Steinberg, Valerie A. Schneider, Tina A. Graves-Lindsay, Robert S. Fulton, Richa Agarwala, John Huddleston, Sergey A. Shiryev, Aleksandr Morgulis, Urvashi Surti, Wesley C. Warren, Deanna M. Church, Evan E. Eichler, and Richard K. Wilson. Single haplotype assembly of the human genome from a hydatidiform mole. *Genome Res*, 24(12):2066–2076, Dec 2014.

[39] Peter H Sudmant, Jacob O Kitzman, Francesca Antonacci, Can Alkan, Maika Malig, Anya Tsalenko, Nick Sampas, Laurakay Bruhn, Jay Shendure, 1000 Genomes Project, and Evan E Eichler. Diversity of human copy number variation and multicopy genes. *Science*, 330(6004):641–646, Oct 2010.

[40] Peter H. Sudmant, Swapan Mallick, Bradley J. Nelson, Fereydoun Hormozdiari, Niklas Krumm, John Huddleston, Bradley P. Coe, Carl Baker, Susanne Nordenfelt, Michael Bamshad, Lynn B. Jorde, Olga L. Posukh, Hovhannes Sahakyan, W. Scott Watkins, Levon Yepiskoposyan, M. Syafiq Abdullah, Claudio M. Bravi, Cristian Capelli, Tor Hervig, Joseph T. S. Wee, Chris Tyler-Smith, George van Driem, Irene Gallego Romero, Aashish R. Jha, Sena Karachanak-Yankova, Draga Toncheva, David Comas, Brenna Henn, Toomas Kivisild, Andres Ruiz-Linares, Antti Sajantila, Ene Metspalu, Jüri

Parik, Richard Villems, Elena B. Starikovskaya, George Ayodo, Cynthia M. Beall, Anna Di Rienzo, Michael F. Hammer, Rita Khusainova, Elza Khusnutdinova, William Klitz, Cheryl Winkler, Damian Labuda, Mait Metspalu, Sarah A. Tishkoff, Stanislav Dryomov, Rem Sukernik, Nick Patterson, David Reich, and Evan E. Eichler. Global diversity, population stratification, and selection of human copy-number variation. *Science*, 349(6253), 2015.

[41] The 1000 Genomes Project Consortium. A global reference for human genetic variation. *Nature*, 526(7571):68–74, Sep 2015.

[42] Helga Thorvaldsdóttir, James T Robinson, and Jill P Mesirov. Integrative Genomics Viewer (IGV): high-performance genomics data visualization and exploration. *Briefings in bioinformatics*, 14:178–192, March 2013.

[43] Beniamino Trombetta and Fulvio Cruciani. Y chromosome palindromes and gene conversion. *Human genetics*, 136:605–619, May 2017.

[44] Eray Tuzun, Andrew J Sharp, Jeffrey A Bailey, Rajinder Kaul, V. Anne Morrison, Lisa M Pertz, Eric Haugen, Hillary Hayden, Donna Albertson, Daniel Pinkel, Maynard V Olson, and Evan E Eichler. Fine-scale structural variation of the human genome. *Nat Genet*, 37(7):727–732, Jul 2005.

[45] Kai Ye, Marcel H Schulz, Quan Long, Rolf Apweiler, and Zemin Ning. Pindel: a pattern growth approach to detect break points of large deletions and medium sized insertions from paired-end short reads. *Bioinformatics*, 25(21):2865–2871, Nov 2009.